Amperometric Detection of Aqueous Silver Ions by Inhibition of Glucose Oxidase Immobilized on Nitrogen-Doped Carbon Nanotube Electrodes

ARTICLE *in* ANALYTICAL CHEMISTRY · JUNE 2015

Impact Factor: 5.64 · DOI: 10.1021/acs.analchem.5b01224 · Source: PubMed

3 AUTHORS, INCLUDING:

Jacob Goran
Instrumentation Laboratory, Bedford, United …

23 PUBLICATIONS **110** CITATIONS

SEE PROFILE

analytical chemistry

Article

pubs.acs.org/ac

Amperometric Detection of Aqueous Silver Ions by Inhibition of Glucose Oxidase Immobilized on Nitrogen-Doped Carbon Nanotube Electrodes

Ian M. Rust,[†] Jacob M. Goran,[†] and Keith J. Stevenson*,[†]

[†]Department of Chemistry, Center for Nano- and Molecular Science and Technology, The University of Texas at Austin, 105 E. 24th St. Stop A5300, Austin, Texas 78712-1224, United States

Supporting Information

ABSTRACT: An amperometric glucose biosensor based on immobilization of glucose oxidase on nitrogen-doped carbon nanotubes (N-CNTs) was successfully developed for the determination of silver ions. Upon exposure to glucose, a steady-state enzymatic turnover rate was detected through amperometric oxidation of the H_2O_2 byproduct, directly related to the concentration of glucose in solution. Inhibition of the steady-state enzymatic glucose oxidase reaction by heavy metals ions such as Ag^+, produced a quantitative decrease in the steady-state rate, subsequently creating an ultrasensitive metal ion biosensor through enzymatic inhibition. The Ag^+ biosensor displayed a sensitivity of $2.00 \times 10^8 \pm 0.06\ M^{-1}$, a limit of detection ($\sigma = 3$) of 0.19 ± 0.04 ppb, a linear range of 20−200 nM, and sample recovery at 101 ± 2%, all acquired at a low-operating potential of 0.05 V (vs Hg/Hg_2SO_4). Interestingly, the biosensor does not display a loss in sensitivity with continued use due to the % inhibition based detection scheme: loss of enzyme (from continued use) does not influence the % inhibition, only the overall current associated with the activity loss. The heavy metals Cu^{2+} and Co^{2+} were also detected using the enzyme biosensor but found to be much less inhibitory, with sensitivities of $1.45 \times 10^6 \pm 0.05\ M^{-1}$ and $2.69 \times 10^3 \pm 0.07\ M^{-1}$, respectively. The mode of GOx inhibition was examined for both Ag^+ and Cu^{2+} using Dixon and Cornish-Bowden plots, where a strong correlation was observed between the inhibition constants and the biosensor sensitivity.

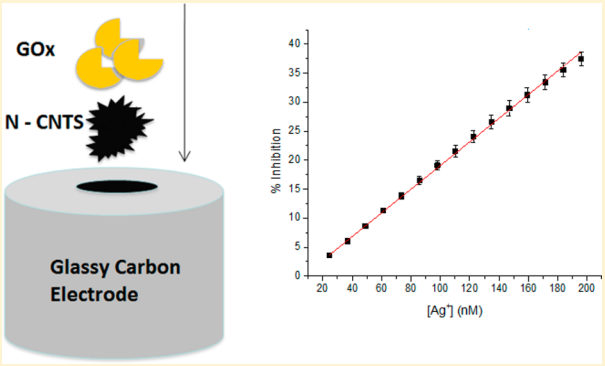

Carbon nanotubes (CNTs) have attracted significant attention as advanced carbon electrode materials[1] for biosensing applications,[2−7] ever since their initial use for dopamine detection.[8] CNTs have been shown to mitigate surface fouling,[2,3,5,9] display electrocatalytic activity toward enzymatic byproducts such as NADH and H_2O_2,[2,3,5] and enhanced enzyme loading[10] due to their increased surface area, particularly for 3D mesh electrodes.[11] CNTs are therefore a terrific candidate for amperometric enzyme inhibition-based biosensing applications. In this type of assay, enzyme inhibitor concentrations (which are typically pesticides or heavy metals) can be measured by monitoring the attenuation of the immobilized enzyme activity. These types of sensors generally exhibit high sensitivities since most enzymes are susceptible to very low concentrations of inhibitors.[12] CNTs have been utilized in only a few studies involving horseradish peroxidase[13] and acetylcholinesterase[14−16] inhibition; however, nitrogen-doped CNTs (N-CNTs), where nitrogen is incorporated into the all carbon lattice, have never before been applied to this type of assay. N-CNTs have been shown to enhance many of the features that make CNTs attractive for biosensing applications.[17] N-CNTs display markedly higher electrocatalytic activity toward enzymatic byproducts NADH and H_2O_2,[18−20] increased protein loading,[21] decreased hydrophobicity,[17,22] and increased biocompatibility.[23,24] N-CNTs are, therefore, an even better candidate for amperometric enzyme inhibition-based biosensing applications.

Glucose oxidase (GOx) is an excellent enzyme for biosensing applications due to its high specificity, high turnover rate, high stability, and low cost.[25] GOx has been successfully paired with N-CNTs in previous work from this group with[26] and without[27] the use of binders for glucose sensing. GOx is known to be inhibited by a number of heavy metals,[25,28,29] including Ag^+, Hg^{2+}, Cu^{2+}, Pb^{2+}, Co^{2+}, Fe^{3+}, and Ni^{2+}, and these interactions have been utilized in numerous GOx-inhibition based heavy metal assays.[29−36] Immobilization of the enzyme is often achieved by polymer or hydrogel entrapment; however, the immobilization matrices in many of these studies are believed to competitively coordinate heavy metal ions, leading to less robust sensors and inconsistent results.[33]

Heavy metal pollution is recognized today as a necessary and important aspect of environmental monitoring. In recognition

Received: March 31, 2015
Accepted: June 16, 2015
Published: June 16, 2015

DOI: 10.1021/acs.analchem.5b01224
Anal. Chem. 2015, 87, 7250−7257

of this, regulatory agencies, such as the WHO and EPA, have set rigid limits on the ranges of permissible heavy metal concentrations.[37] Current methods of analyzing heavy metals, such as flame atomic absorption spectroscopy (FAAS) or inductively coupled plasma-atomic emission spectroscopy (ICP-AES), are reliable but are also expensive and require cumbersome equipment. This approach hinders analysis in areas where heavy metal exposure is most prominent: less-developed countries.[38] Furthermore, these bulky analytical systems lack portability, precluding the opportunity to quantify heavy metals at the sample acquisition point.

The environmental presence of one metal, in particular, silver, is a growing concern as a result of the increasing utilization of silver and silver compounds in medicine and industrial applications. Since silver ions cause acute toxicity to aquatic species, the fast and reliable detection of trace amounts of aqueous silver in industrial and environmental water samples is of considerable importance.[39] Silver is also intimately associated with the environmental contamination of other toxic metals such as lead and mercury. Electrochemical detection of heavy metals offers a cheap, portable, and relatively simple alternative to spectroscopic methods. Thus, Ag^+ biosensors,[29,33,40−44] chemosensors,[45−47] ion-selective electrodes,[48,49] and voltammetric techniques[49−51] are currently being investigated. Herein, we present a simple, cost-effective, and highly sensitive approach to heavy metal detection, focusing on silver in particular. N-CNTs are coupled with physically adsorbed GOx to demonstrate an enzyme inhibition-based heavy metals detection scheme. An investigation of the mode of inhibition and inhibition constants for several GOx-inhibiting heavy metals is also included.

EXPERIMENTAL SECTION

Enzyme and Chemicals. Glucose oxidase (Type X-S from *Aspergillus niger*, E.C. 1.1.3.4, lyophilized powder, 100−250 U/mg, MW 160 kDa), α-D-glucose (96%), and cobalt chloride ($CoCl_2$) were purchased from Sigma-Aldrich. Cupric nitrate [$Cu(NO_3)_2$], sodium hydroxide (NaOH), pyridine, sodium phosphate monobasic (NaH_2PO_4, monohydrate), and sodium phosphate dibasic (Na_2HPO_4, anhydrous) were purchased from Fisher. Silver nitrate ($AgNO_3$) was acquired from Acros. Bis(cyclopentandienyl) iron (ferrocene, 99%) was obtained from Alfa Aesar. Ethylenediaminetetraacetic acid (EDTA) was purchased from EM Science. Ethanol (anhydrous) was purchased from Pharmco-AAPER. Ultrapure water (≥18 MΩ cm) was used throughout.

N-CNT Synthesis. N-CNTs were synthesized via a chemical vapor deposition (CVD) process where N-CNTs were produced using a 20 mg/mL ferrocene in pyridine solution injected within a quartz tube spanning two identical tube furnaces (Carbolite model HST 12/35/200/2416CG), as described in previous work from this group.[26,52,53] N-CNTs made by this process have been characterized extensively by X-ray photoelectron spectroscopy[52,53] and are known to have 7.4 ± 0.5 atom % nitrogen.

Biosensor Construction. Synthesized N-CNTs were mixed with absolute ethanol to form a 2 mg/mL solution, which was sonicated (Branson ultrasonic cleaner, model 2510R-MTH) for 2 h to ensure a homogeneous solution. A single 12 μL aliquot of the N-CNT/ethanol solution (24 μg of N-CNTs) was drop-cast onto the prepolished surface of 0.5 cm diameter glassy carbon (GC) rotating disk electrodes (RDEs), PINE Instruments AFE2M050GC, and allowed to dry completely. Binders, dispersion agents/surfactants, and oxidizing agents were not used in the construction of the biosensors. GC-RDEs were polished, prior to drop-casting, with 0.05 μm alumina slurry on microcloth (Buehler) and sonicated in ultrapure water for one to 2 min to remove adsorbed alumina. Once dried, the drop-cast RDEs were "wet" with a mixture of 0.1 M sodium phosphate buffer (SPB) at pH 7.0 and ethanol (1:20, ethanol: buffer, by volume). The wet electrodes were submerged in a 0.1 mg/mL solution of GOx in 0.1 M SPB for exactly 2 min, to allow the adsorption of GOx onto the N-CNTs at room temperature. Electrodes were rinsed with SPB to remove any loosely adsorbed GOx before use.

Electrochemistry. A three-electrode cell consisting of the biosensor described above, a coiled Au counter electrode, and a Hg_2SO_4 reference electrode (CH Instruments, +0.64 V vs SHE) were used in conjunction with a five-neck 125 mL glass cell for all electrochemical experiments. The RDEs were placed in a Pine Instruments AFMSRX analytical rotator and set at a rate of 4000 rpm, unless stated otherwise. Chronoamperometric measurements were taken with an Autolab PGSTAT30 potentiostat (Autolab GPES software, version 4.9) poised at +0.05 V vs Hg_2SO_4. At this potential, the enzymatically generated H_2O_2 is oxidized, thus, the observed oxidative current (caused by the presence of glucose) is a measure of the enzymatic activity of adsorbed GOx. This potential also represents the lowest potential with the highest oxidative current response to H_2O_2 at N-CNT electrodes; higher potentials do not appreciably increase the sensitivity.[54]

For the final biosensing parameters, a 2 mL aliquot of 2.5 M glucose (in 0.1 M SPB, pH 7.0) was introduced to the cell, resulting in a steady-state oxidative current defined as I_0. Metal inhibitor solutions (prepared in water, due to the poor solubility of metal-phosphate compounds) were then introduced in small aliquots and the current response, termed I, was recorded. In order to ensure the steady-state current response was achieved after metal ion injection, a period of 200 s was allowed to elapse between metal ion additions. The inhibition percentage at each metal ion concentration was calculated using the expression shown below (eq 1):

$$\text{Inh}\% = \frac{[I_0 - I]}{I_0} \times 100\% \quad (1)$$

The resulting % inhibition can be plotted versus molar inhibitor concentration to create a heavy metal assay with sensitivity units of M^{-1}.

RESULTS AND DISCUSSION

Optimization of the Operating Substrate Concentration. The substrate concentration utilized during the operation of enzyme inhibition-based biosensors is known to have a profound effect on the overall analytical performance,[55] especially in the case of uncompetitive and mixed-type inhibition, where the inhibitor binds to the enzyme−substrate complex. There is not a clear consensus on the optimal substrate concentration for biosensor operation, as previous studies utilizing GOx for enzyme inhibition-based biosensors range from as low as 0.2 mM to as high as 40 mM glucose.[29,30,32,33] Although the initial current, I_0, is directly proportional to the concentration of substrate, the influence of substrate concentration on the enzyme's sensitivity to an inhibitor is less straightforward. Thus, we examined the sensitivity of the biosensor to Ag^+ as a function of the glucose

DOI: 10.1021/acs.analchem.5b01224
Anal. Chem. 2015, 87, 7250−7257

concentrations from 5 to 200 mM, shown in Figure 1. The sensor's sensitivity to Ag^+ increases concomitantly with glucose concentration until around 50 mM, where the sensitivity appears to plateau.

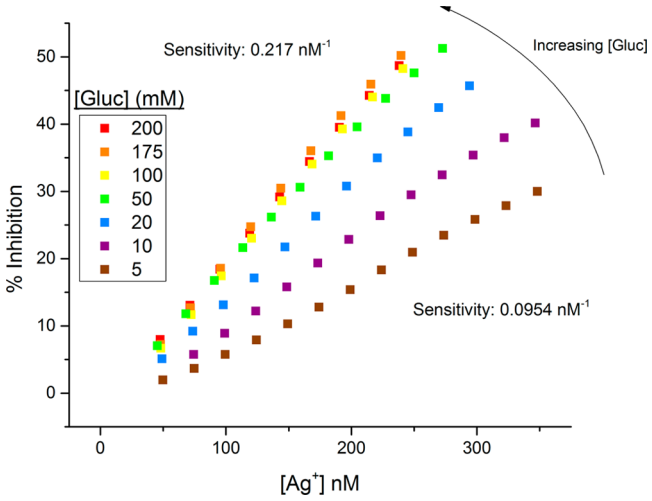

Figure 1. % Inhibition as a function of inhibitor concentration operated at various initial glucose concentrations.

This type of behavior is analogous to the well-known Michaelis–Menten (MM) model for enzyme kinetics, which also shows a plateau in the enzymatic activity as a function of substrate concentration. A plot of the N-CNT/GOx biosensor's activity as a function of glucose concentration (a Michaelis–Menten plot) is shown in Figure 2A, while a plot of the N-CNT/GOx biosensor's sensitivity to Ag^+ as a function of glucose concentration is shown in Figure 2B. MM plots relate the enzyme's catalytic rate to the concentration of substrate and are often used to determine the Michaelis constant, K_m, the substrate concentration at which the reaction rate is at half-maximum. The apparent K_m, K_m^{app}, was determined from fitting of the MM curve and found to be 24.5 ± 0.4 mM glucose, while GOx saturation (where the MM curve begins to plateau significantly) occurs around twice that value, or approximately 50 mM, the same concentration at which the sensitivity to Ag^+ reached its maximum plateau. This suggests that GOx is most sensitive to Ag^+ inhibition when it becomes saturated with glucose, any additional glucose after saturation will increase its sensitivity minimally, if at all. An operating glucose concentration of 50 mM was used exclusively in future studies.

Response Time. Due to the nature of inhibition, enzyme inhibition-based biosensors tend to have fairly sluggish response times, especially when compared to conventional direct-monitoring amperometric biosensors, which can exhibit nearly instantaneous responses.[56] Previous heavy metal enzyme inhibition-based biosensors have reported response times, defined as the time required to reach steady-state after introduction of the inhibitor, on the order of several minutes[29,30,57] or longer,[58] but often are unreported.[33] In some cases, especially those with irreversible inhibition, the biosensor is incubated in inhibitor solution for several minutes (often 10 min+) at each step in the calibration curve.[13,40] This technique can result in faster response times and lower detection limits; however, the incubation time must also be considered in the overall biosensor performance. In this work, the total time is taken into account, as several parameters (vide infra) were investigated using response time as a differentiating metric, subsequently forming a functional enzyme inhibition-based biosensor.

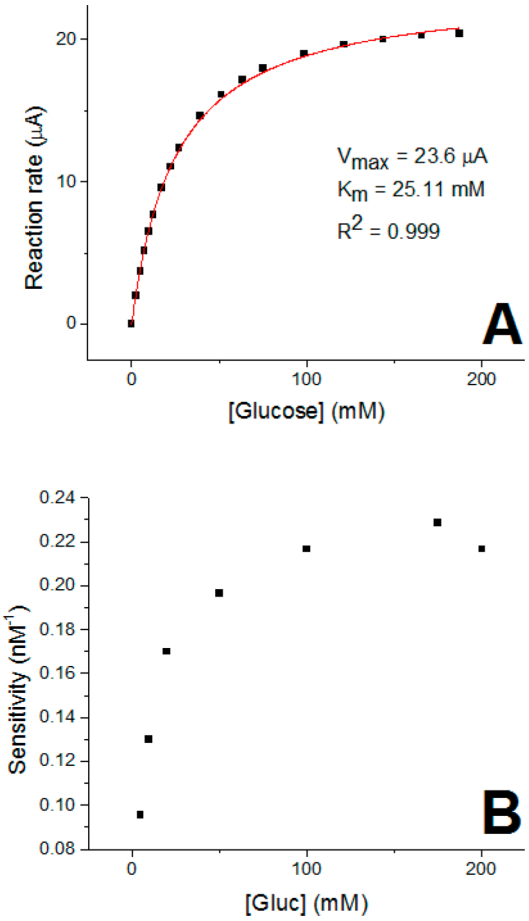

Figure 2. (A) A representative Michaelis–Menten curve for GOx obtained with a GOx/N-CNT biosensor and (B) the sensitivity of the N-CNT/GOx biosensors to Ag^+ as a function of the operating glucose concentration (0.1 M SPB, pH 7.0, rotation rate 4000 rpm). V_{max} is the maximum rate achieved by the system.

Optimization of the Concentration of GOx During Adsorption. The concentration of the GOx solution used for spontaneous adsorption onto the N-CNT modified GC electrode was varied from 0.1 mg/mL to 50 mg/mL, in order to determine its effect on response time to Ag^+ inhibition. For all GOx concentrations, N-CNTs were placed in solution for exactly 30 seconds. Figure 3 displays the drop in enzymatic activity for a single 5 μM addition of Ag^+, introduced into solution at t = 240 s. It is clear from Figure 3 that the amount of GOx adsorbed on the surface of the electrode plays a significant role in the inhibitive response time. Lower concentrations of GOx, where there is less GOx adsorbed on the N-CNT surface, result in a much faster response time (less than 200 s), whereas the 50 mg/mL bioelectrode took nearly 700 s to reach steady-state after the introduction of silver. At concentrations less than 0.1 mg/mL, attenuation of I_0 after Ag^+ introduction becomes impossible to discern from noise and are therefore not shown. In order to achieve the fastest response time possible, 0.1 mg/mL was selected as the optimal GOx adsorption concentration.

Optimization of the Adsorption Time. Since GOx adsorption onto N-CNT electrodes most likely obeys the same Langmuir adsorption isotherm characteristics as its

DOI: 10.1021/acs.analchem.5b01224
Anal. Chem. 2015, 87, 7250–7257

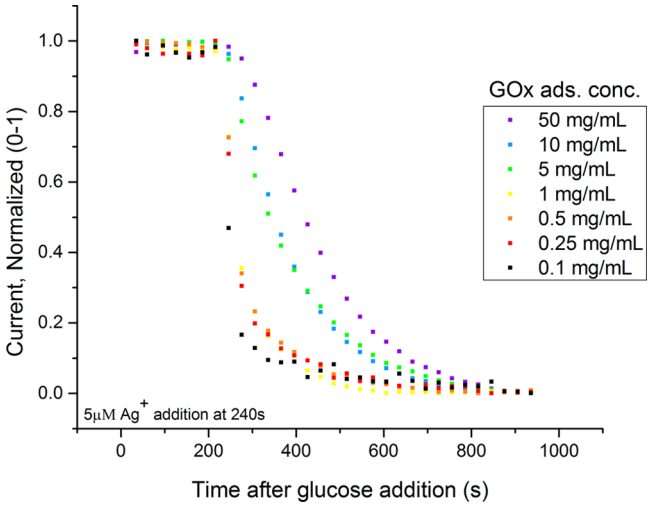

Figure 3. Variation in biosensor response time as a function of the GOx concentration used during adsorption. Current is normalized to I_0 and I, where I_0 is 1 and I, the final steady-state current after the introduction of inhibitor, is 0 (0.1 M SPB, pH 7.0, operating glucose concentration at 50 mM glucose, 5 μM of silver introduced at t = 240 s, rotation rate 4000 rpm).

cofactor, flavin adenine dinucleotide (FAD), the length of time the electrodes are allowed to adsorb will also dictate the amount of GOx adsorbed but contribute less of a role than the adsorption concentration.[27] In Figure 4, the amount of time N-

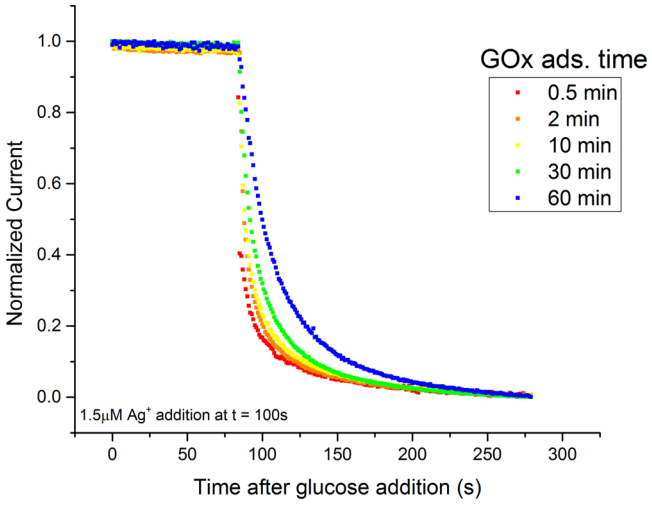

Figure 4. Variation in biosensor response time as a function of adsorption time in a 0.1 mg/mL GOx solution. Current is normalized to I_0 and I, where I_0 is 1 and I, the final steady-state current after the introduction of inhibitor, is 0 (0.1 M SPB, pH 7.0, operating glucose concentration at 50 mM glucose, 1.5 μM of silver introduced at t = 240 s, rotation rate 4000 rpm).

CNTs were allowed to adsorb from a 0.1 mg/mL GOx solution was varied from 0.5−60 min. Similar to the adsorption concentration optimization study, shorter adsorption periods (less adsorbed enzyme) here resulted in faster response times. As expected, the effect of adsorption time is not as marked as that seen in Figure 3. In fact, the shortest two time periods display nearly identical response times. The 2 min time period was selected over 0.5 min in order to improve reproducibility (any slight variations in the adsorption time would have a smaller relative effect at 2 min than at 0.5 min).

Optimization of the Rotation Rate. Figure 5A presents a single 500 nM addition of Ag^+ introduced to GOx/N-CNT

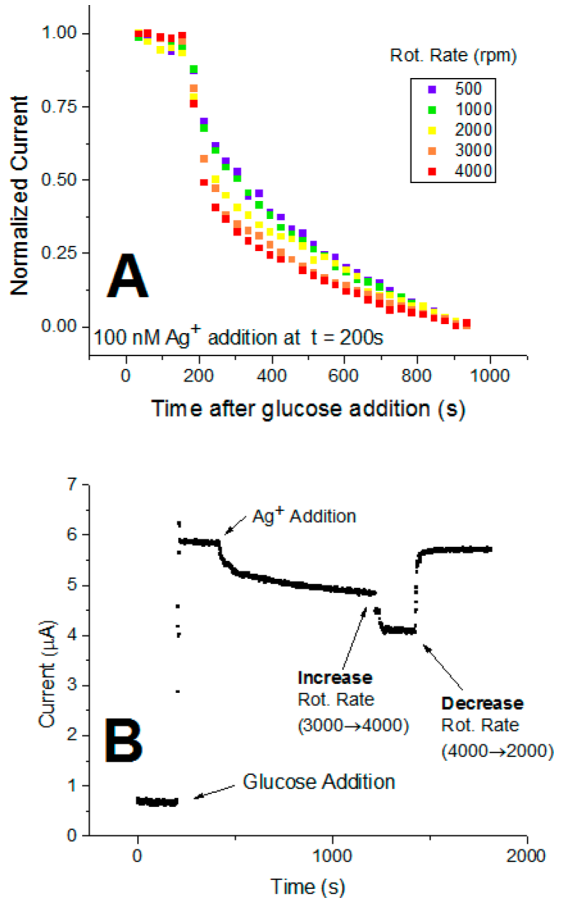

Figure 5. (A) Variation in biosensor response time with RDE's rotation rate. Current is normalized between 0 and 1, where I_0 is 1 and I is 0. A single, 50 mM addition of glucose at t = 0 was followed by an addition of silver at t = 200 s. (B) Rotating disk chronoamperogram in which the rotation rate was varied midrun (0.1 M SPB, pH 7.0).

bioelectrodes as a function of rotation rate from 500 to 4000 rpm. As the rotation rate increases, inhibition of the enzymatic activity occurs faster, especially in the first few seconds after the introduction of inhibitor. The increase in the enzyme inhibition response time can be attributed to the increase in mass transport of Ag^+ ions at higher rotation rates. Surprisingly, an increase in the rotation rate will also cause a decrease in the overall current, and conversely, a decrease in rotation rate will induce a significant increase in the overall current. A chronoamperogram is shown in Figure 5B, where, after the introduction of a single 100 nM Ag^+ addition, the rotation rate was increased, with a subsequent decrease in the overall current. Figure 5B also shows, within the same chronoamperogram, a decrease in the rotation rate, which subsequently increases the overall current. This type of response is counterintuitive, as one would expect the current from an electroactive species in solution to obey the Levich equation,[59] which provides the current at a rotating disk electrode, shown below (eq 2):

$$I_L = (0.620)nFAD^{2/3}\omega^{1/2}\nu^{-1/6}C \quad (2)$$

DOI: 10.1021/acs.analchem.5b01224
Anal. Chem. 2015, 87, 7250−7257

Where I_L is the mass transport limited current, n is the number of electrons transferred, F is Faraday's constant (96485 C/mol), D is the diffusion coefficient of the electroactive species, ω is the angular velocity ($2\pi f$, where f is frequency), ν is the kinematic viscosity of the solvent (0.01 cm^2/s for water), and C is the concentration of the electroactive species. According to the Levich equation, IL will increase with rotation rate to the one-half power. The decreased current observed in this case can be attributed to a decrease in the residence time, since the electroactive molecule, H_2O_2, is being enzymatically generated at the N-CNT surface, where it is also electrochemically detected. Thus, although the enzymatic substrate and inhibitor will display increased mass transport as a function of the rotation rate, the detected oxidation current from H_2O_2 will be decreased, since it will be carried away from the N-CNT surface at a faster rate with higher rotation rates and have less residence time to be electrochemically oxidized at the N-CNT surface. It should be noted that the shift in the overall current as a function of rotation rate was observed before or after the introduction of Ag^+, even though Figure 5B only displays the change after Ag^+ was introduced. Although more total current could be achieved at lower rotation rates, the fastest rotation rate of 4000 rpm was selected, in order to minimize the biosensor's response time.

Metal Ion Detection and Analytical Figures of Merit. The final biosensor parameters consisted of 2 min of adsorption in a 0.1 mg/mL solution of GOx, an operating glucose concentration of 50 mM, and a rotation rate of 4000 rpm. The biosensors displayed a linear range for Ag^+ from approximately 20−200 nM ($R^2 \geq 0.999$), using 12.25 nM additions of Ag^+. Representative chronoamperograms displaying the current response to Ag^+ as a function of time are shown in Figure S-1 of the Supporting Information. Although the design of this enzyme inhibition-based biosensor was tailored to minimize the response time, 200 s were allowed to elapse between each addition, in order to ensure the response consistently reached steady-state. The calibration curve, featured in Figure 6,

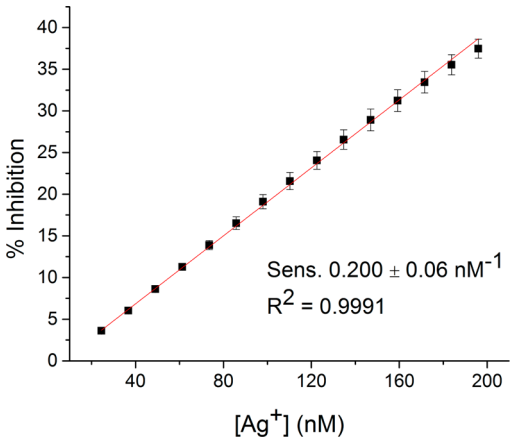

Figure 6. Average Ag^+ calibration curve from the proposed inhibition-based sensor. Error bars are 95% confidence limits.

possesses a sensitivity of $2.00 \times 10^8 \pm 0.06$ M^{-1} which, to our knowledge, is the highest reported value for this type of sensor to date.[33] The limit of detection (LOD), defined as 3σ/sensitivity, was determined to be 1.8 ± 0.4 nM, and is the lowest reported among Ag^+ enzyme inhibition-based biosensors[29,33,40−44,60] and comparable to other recently published potentiometric (LOD: 4.17 nM,[48] 0.9 nM[49]) and voltammetric (LOD: 1.2 nM,[49] 1.5 nM,[50] 1.3 nM[51]) techniques. For evaluation of the working biosensors accuracy, recovery tests were also completed on 100 nM Ag^+ standards, with an average recovery of 101 ± 2%. Table 1 shows the analytical figures of merit with comparisons to other chronoamperometric enzyme inhibition-based Ag^+ sensors.

Repeatability for a single electrode was determined from six individually prepared 150 nM Ag^+ samples with a wash of the electrode between each measurement. Two different types of washes were employed: (1) a simple phosphate buffer wash and (2) a wash in phosphate buffer solution saturated with EDTA. The repeatability values were 2.8% and 1.6% RSD, respectively; however, the two sets of six measurements were not statistically different, so EDTA does not appear to be necessary for biosensor restoration. Interestingly, no loss in sensitivity was observed over the course of the six measurements. Although there was a slight loss in adsorbed enzyme with each use (as evidenced by a slight diminution of I_0), the percent inhibition of the remaining enzyme by Ag^+ (and therefore the sensitivity) remained unchanged. Thus, the amount of adsorbed enzyme does not affect the sensitivity, provided measurements are plotted in % inhibition versus inhibitor concentration. Additionally, the linear range of the Ag^+ sensor can be tuned by adjusting the operating glucose concentration. For example, the linear range for a biosensor operating in a very low (2 mM) concentration of glucose will be 100−800 nM Ag^+, as displayed in Figure S-2 of the Supporting Information.

The GOx/N-CNT biosensor was evaluated with two other metal ions, Cu^{2+} and Co^{2+}, and the resulting % inhibition vs inhibitor concentration plots are shown in Figure 7 (panels A and B, respectively). Unlike silver, these measurements were made in pH 6.0 acetate buffer, due to the extreme insolubility of $Cu_3(PO_4)_2$ and $Co_3(PO_4)_2$. The biosensor was more than 2 orders of magnitude less sensitive to Cu^{2+} (slope: $1.45 \pm 0.05 \times 10^6$ M^{-1}) and nearly 5 orders of magnitude less sensitive to Co^{2+} (slope: $2.69 \pm 0.07 \times 10^3$ M^{-1}) compared to Ag^+.

Investigation of the Inhibition Mode and Determination of the Inhibition Constant. The mechanisms of Ag^+ and Cu^{2+} inhibition of GOx were determined through Dixon and Cornish-Bowden (CB) plots, shown in Figure S-3 of the Supporting Information. The combination of these linearized graphing methods allows for a relatively straightforward deduction of both the inhibition mode and the value of the related inhibition constants, K_i and K_i'.[61] K_i is the dissociation constant of the enzyme−inhibitor complex, while K_i' is the dissociation constant of the enzyme−substrate−inhibitor complex (and therefore only associated with uncompetitive, mixed, and noncompetitive inhibition). For both K_i and K_i', smaller values indicate a stronger interaction with the inhibitor. Both Ag^+ and Cu^{2+} were found to inhibit GOx with a mixed-type interaction (meaning the metal ion binds to both the enzyme and the enzyme−substrate complex) as illustrated by the single point of intersection observed in the Dixon and CB plots. This mode of inhibition is in agreement with previous work.[29,32,33,62] This analysis was not extended to Co^{2+} due to the biosensor's meager sensitivity toward this metal ion, making these linearization techniques unworkable.

The inhibition constants for Ag^+, determined from these points of intersection, were found to be $K_i = 700 \pm 9$ nM and $K_i' = 106 \pm 5$ nM; the constants for Cu^{2+} were $K_i = 84 \pm 3$ μM and $K_i' = 23.3 \pm 0.7$ μM. These values indicate that these metal ions bind much more strongly to the GOx−glucose complex

DOI: 10.1021/acs.analchem.5b01224
Anal. Chem. 2015, 87, 7250−7257

Table 1. Comparison of Analytical Figures of Merit for Ag^+ Enzyme-Inhibition Based Sensors[a]

sensor	sensitivity (M^{-1})	% RSD	limit of detection (nM)	linear range (nM)	operating potential (V vs Hg/Hg_2SO_4)	reference
N-CNT/GOx	2.00×10^8	3.1	1.8	20−200	0.05	this work
$Au/GOx_{solution}$	1.22×10^7	7.0	2	2−40	0.33	33[b]
	1.23×10^6	5.2		40−300		
Au/GOx_{ads}	4.25×10^6	2.5	8	10−120	0.33	33
	8.3×10^5	4.0		120−600		
Au/PNA/GOx	8.93×10^6	4.6	5	10−60	0.33	33
	2.03×10^6	5.6		60−300		
Pt/PPD/GOx	[c]	3.5	50	50−400	0.33	29
Pt/AGG/Invertase	NR	NR	50	50−500	−0.07	40

[a]NR: not reported. PNA: poly(L-noradrenalin). PPD: poly *o*-phenylenediamine AGG: agarose−guar gum. [b]Authors reported two, separate linear ranges for each sensor. [c]Constructed calibration curves of 1/current vs concentration. Sensitivity was 11.83 μA^{-1} μM^{-1}.

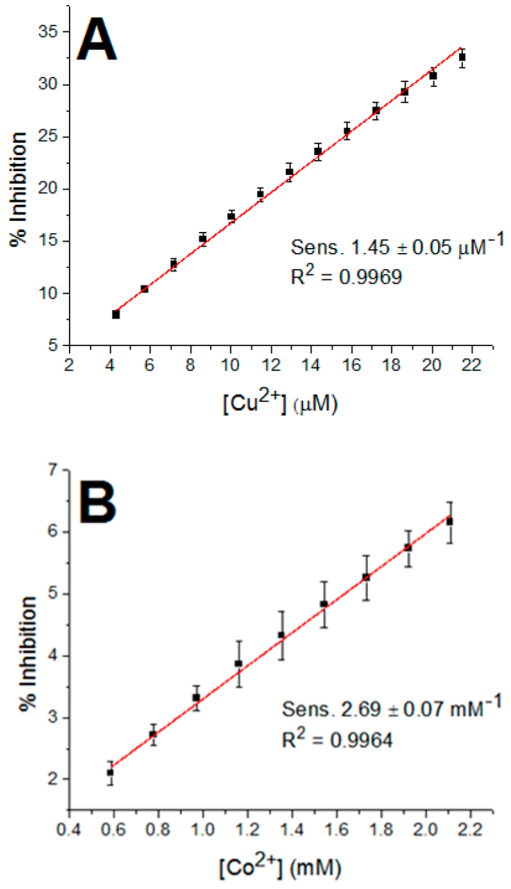

Figure 7. % Inhibition vs inhibitor concentration plots for (A) Cu^{2+} and (B) Co^{2+} (0.1 M acetate buffer, pH 6.0, error bars are 95% confidence limits).

than to GOx alone. This is most likely why the biosensor's sensitivity to silver grew significantly as the operating glucose concentration was increased. Additionally, the substantial (2 orders of magnitude) difference between the biosensor's sensitivity to Ag^+ and Cu^{2+} is mirrored by a comparably large difference in the inhibition constants.

N-CNT Coordination of Silver Ions. While oxidized/functionalized CNT sheets have been previously used as an adsorbent material for heavy metals in solution,[63−65] there is no published work, to our knowledge, concerning the metal ion adsorption properties of N-CNTs. To determine if Ag^+ adsorption was occurring on the N-CNTs, an N-CNT electrode (without adsorbed GOx) was submerged in a 1.0 μM solution of Ag^+ (four times the highest Ag^+ concentration in the sensor's linear range), for a period of 30 min. Cyclic voltammograms, cycled to a high negative potential (−1.4 V) in order to first reduce any Ag^+ present, were obtained before and after the adsorption period. As seen in Figure 8, a silver anodic

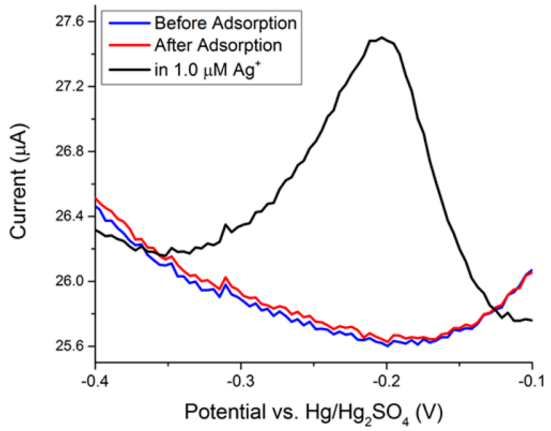

Figure 8. Selected portion of CV highlighting the silver stripping peak around −0.20 V. CVs were cycled between +0.2 V and −1.4 V in pH 7.0, 0.1 M SPB at a scan rate of 10 mV/s.

stripping peak will occur at −0.20 V versus Hg/Hg_2SO_4, and the presence of such a peak would indicate adsorbed Ag^+. However, even after adsorption in a high Ag^+ concentration, adsorbed Ag^+ was not detected (Figure 8).

CONCLUSION

N-CNTs have been paired with spontaneously adsorbed GOx to create a simple, yet highly sensitive biosensor for aqueous silver ions. The biosensor displayed a $2.00 \times 10^8 \pm 0.06$ M^{-1} sensitivity toward Ag^+, the highest reported sensitivity for a sensor of this type, attributed to the extremely high electrocatalytic activity of N-CNTs toward enzymatically generated H_2O_2. The sensor also displayed a detection limit of 1.8 ± 0.4 nM and a linear range of 20−200 nM, with an optimized response time of less than 200 s. Repeated use of the sensor did not result in a loss of sensitivity, nor did the N-CNTs appreciably adsorb Ag^+. For these reasons, the enzyme inhibition-based biosensor presented here is a promising candidate for environmental metal ion monitoring and toxicity testing.

DOI: 10.1021/acs.analchem.5b01224
Anal. Chem. 2015, 87, 7250−7257

■ ASSOCIATED CONTENT

Supporting Information

Three graphs as noted in text. The Supporting Information is available free of charge on the ACS Publications website at DOI: 10.1021/acs.analchem.5b01224.

■ AUTHOR INFORMATION

Corresponding Author

*E-mail: Stevenson@cm.utexas.edu.

Notes

The authors declare no competing financial interest.

■ ACKNOWLEDGMENTS

Financial support of this work was provided by the R.A. Welch Foundation (Grant F-1529).

■ REFERENCES

(1) McCreery, R. L. *Chem. Rev.* **2008**, *108*, 2646−2687.
(2) Wang, J. *Electroanalysis* **2005**, *17*, 7−14.
(3) Vashist, S. K.; Zheng, D.; Al-Rubeaan, K.; Luong, J. H. T.; Sheu, F.-S. *Biotechnol. Adv.* **2011**, *29*, 169−188.
(4) Rubianes, M.; Rivas, G. *Electroanalysis* **2005**, *17*, 73−78.
(5) Lin, Y.; Yantasee, W.; Wang, J. *Front. Biosci.* **2005**, *10*, 582.
(6) Jacobs, C. B.; Peairs, M. J.; Venton, B. J. *Anal. Chim. Acta* **2010**, *662*, 105−127.
(7) Balasubramanian, K.; Burghard, M. *Anal. Bioanal. Chem.* **2006**, *385*, 452−468.
(8) Britto, P. J.; Santhanam, K. S. V.; Ajayan, P. M. *Bioelectrochem. Bioenerg.* **1996**, *41*, 121−125.
(9) Swamy, B. E. K.; Venton, B. J. *Analyst* **2007**, *132*, 876.
(10) Feng, W.; Ji, P. *Biotechnol. Adv.* **2011**, *29*, 889−895.
(11) Nejadnik, M. R.; Deepak, F. L.; Garcia, C. D. *Electroanalysis* **2011**, *23*, 1462−1469.
(12) Bachan Upadhyay, L. S.; Verma, N. *Anal. Lett.* **2013**, *46*, 225−241.
(13) Moyo, M.; Okonkwo, J. O. *Sens. Actuators, B* **2014**, *193*, 515−521.
(14) Cai, J.; Du, D. *J. Appl. Electrochem.* **2008**, *38*, 1217−1222.
(15) Chai, Y.; Niu, X.; Chen, C.; Zhao, H.; Lan, M. *Anal. Lett.* **2013**, *46*, 803−817.
(16) Xue, R.; Kang, T.-F.; Lu, L.-P.; Cheng, S.-Y. *Appl. Surf. Sci.* **2012**, *258*, 6040−6045.
(17) Majeed, S.; Zhao, J.; Zhang, L.; Anjum, S.; Liu, Z.; Xu, G. *Nanotechnol. Rev.* **2013**, *2*, 615−635.
(18) Tang, Y.; Allen, B. L.; Kauffman, D. R.; Star, A. *J. Am. Chem. Soc.* **2009**, *131*, 13200−13201.
(19) Xu, X.; Jiang, S.; Hu, Z.; Liu, S. *ACS Nano* **2010**, *4*, 4292−4298.
(20) Goran, J. M.; Favela, C. A.; Stevenson, K. J. *Anal. Chem.* **2013**, *85*, 9135−9141.
(21) Burch, H. J.; Contera, S. A.; de Planque, M. R. R.; Grobert, N.; Ryan, J. F. *Nanotechnology* **2008**, *19*, 384001.
(22) Goran, J. M.; Stevenson, K. J. *Langmuir* **2013**, *29*, 13605−13613.
(23) Carrero-Sánchez, J. C.; Elías, A. L.; Mancilla, R.; Arrellín, G.; Terrones, H.; Laclette, J. P.; Terrones, M. *Nano Lett.* **2006**, *6*, 1609−1616.
(24) Zhao, M. L.; Li, D. J.; Yuan, L.; Yue, Y. C.; Liu, H.; Sun, X. *Carbon* **2011**, *49*, 3125−3133.
(25) Wilson, R.; Turner, A. P. F. *Biosens. Bioelectron.* **1992**, *7*, 165−185.
(26) Lyon, J. L. L.; Stevenson, K. J. *ECS Trans.* **2009**, *16*, 1−12.
(27) Goran, J. M.; Mantilla, S. M.; Stevenson, K. J. *Anal. Chem.* **2013**, *85*, 1571−1581.
(28) Nakamura, S.; Ogura, Y. *J. Biochem. (Tokyo)* **1968**, *64*, 439−447.
(29) Guascito, M. R.; Malitesta, C.; Mazzotta, E.; Turco, A. *Sens. Actuators, B* **2008**, *131*, 394−402.
(30) Samphao, A.; Rerkchai, H.; Jitcharoen, J.; Nacapricha, D.; Kalcher, K. *Int. J. Electrochem Sci.* **2012**, *7*, 1001−1010.
(31) Malitesta, C.; Guascito, M. R. *Selected Papers from the Eighth World Congress on Biosensors Part I* **2005**, *20*, 1643−1647.
(32) Ghica, M. E.; Brett, C. M. A. *Microchim. Acta* **2008**, *163*, 185−193.
(33) Chen, C.; Xie, Q.; Wang, L.; Qin, C.; Xie, F.; Yao, S.; Chen, J. *Anal. Chem.* **2011**, *83*, 2660−2666.
(34) Zeng, G.-M.; Tang, L.; Shen, G.-L.; Huang, G.-H.; Niu, C.-G. *Int. J. Environ. Anal. Chem.* **2004**, *84*, 761−774.
(35) Liu, C. C.; Fryburg, F. M.; Chen, A. K. *Bioelectrochem. Bioenerg.* **1981**, *8*, 703−708.
(36) Liu, J.; Xu, X.; Tang, L.; Zeng, G. *Trans. Nonferrous Met. Soc. China* **2009**, *19*, 235−240.
(37) World Health Organization. *Guidelines for Drinking-Water Quality*; World Health Organization: Geneva, 2011.
(38) Fu, F.; Wang, Q. *J. Environ. Manage.* **2011**, *92*, 407−418.
(39) Howe, P. D.; Dobson, S.; World Health Organization. *Silver and Silver Compounds*; World Health Organization: Geneva, 2002.
(40) Bagal-Kestwal, D.; Karve, M. S.; Kakade, B.; Pillai, V. K. *Biosens. Bioelectron.* **2008**, *24*, 657−664.
(41) Komaba, S.; Fujino, Y.; Matsuda, T.; Osaka, T.; Satoh, I. *Sens. Actuators, B* **1998**, *52*, 78−83.
(42) Soldatkin, A. P.; Volotovsky, V.; El'Skaya, A. V.; Jaffrezic-Renault, N.; Martelet, C. *Anal. Chim. Acta* **2000**, *403*, 25−29.
(43) Soldatkin, O. O.; Kucherenko, I. S.; Pyeshkova, V. M.; Kukla, A. L.; Jaffrezic-Renault, N.; El'skaya, A. V.; Dzyadevych, S. V.; Soldatkin, A. P. *Bioelectrochemistry* **2012**, *83*, 25−30.
(44) Krizkova, S.; Huska, D.; Beklova, M.; Hubalek, J.; Adam, V.; Trnkova, L.; Kizek, R. *Environ. Toxicol. Chem.* **2010**, *29*, 492−496.
(45) Cui, W.; Wang, L.; Xiang, G.; Zhou, L.; An, X.; Cao, D. *Sens. Actuators, B* **2015**, *207* (PartA), 281−290.
(46) Xiang, G.; Cui, W.; Lin, S.; Wang, L.; Meier, H.; Li, L.; Cao, D. *Sens. Actuators, B* **2013**, *186*, 741−749.
(47) Zhang, J. F.; Zhou, Y.; Yoon, J.; Kim, J. S. *Chem. Soc. Rev.* **2011**, *40*, 3416−3429.
(48) Afkhami, A.; Shirzadmehr, A.; Madrakian, T.; Bagheri, H. *Talanta* **2015**, *131*, 548−555.
(49) Shamsipur, M.; Hashemi, B.; Dehdashtian, S.; Mohammadi, M.; Gholivand, M. B.; Garau, A.; Lippolis, V. *Anal. Chim. Acta* **2014**, *852*, 223−235.
(50) Zhang, Z.; Yan, J. *Sens. Actuators, B* **2014**, *202*, 1058−1064.
(51) Yan, G.; Wang, Y.; He, X.; Wang, K.; Su, J.; Chen, Z.; Qing, Z. *Talanta* **2012**, *94*, 178−183.
(52) Maldonado, S.; Morin, S.; Stevenson, K. J. *Carbon* **2006**, *44*, 1429−1437.
(53) Wiggins-Camacho, J. D.; Stevenson, K. J. *J. Phys. Chem. C* **2011**, *115*, 20002−20010.
(54) Goran, J. M.; Phan, E. N. H.; Favela, C. A.; Stevenson, K. J. *Anal. Chem.* **2015**, *87*, 5989−5996.
(55) Arduini, F.; Amine, A.; Moscone, D.; Palleschi, G. *Anal. Lett.* **2009**, *42*, 1258−1293.
(56) Goran, J. M.; Lyon, J. L.; Stevenson, K. J. *Anal. Chem.* **2011**, *83*, 8123−8129.
(57) Attar, A.; Emilia Ghica, M.; Amine, A.; Brett, C. M. A. *J. Hazard. Mater.* **2014**, *279*, 348−355.
(58) Luque de Castro, M. .; Herrera, M. *Biosens. Bioelectron.* **2003**, *18*, 279−294.
(59) Bard, A. J.; Faulkner, L. R. *Electrochemical Methods and Applications*; Wiley-Interscience: New York, 2000.
(60) Kuswandi, B. *Anal. Bioanal. Chem.* **2003**, *376*, 1104−1110.
(61) Cornish-Bowden, A. *Biochem. J.* **1974**, *137*, 143−144.
(62) Toren, E. C., Jr; Burger, F. J. *Microchim. Acta* **1968**, *56*, 538−545.
(63) Ding, Q.; Liang, P.; Song, F.; Xiang, A. *Sep. Sci. Technol.* **2006**, *41*, 2723−2732.
(64) Grazhulene, S. S.; Red'kin, A. N.; Telegin, G. F.; Bazhenov, A. V.; Fursova, T. N. *J. Anal. Chem.* **2010**, *65*, 682−689.

DOI: 10.1021/acs.analchem.5b01224
Anal. Chem. 2015, 87, 7250−7257

(65) Tofighy, M. A.; Mohammadi, T. *J. Hazard. Mater.* **2011**, *185*, 140−147.

DOI: 10.1021/acs.analchem.5b01224
Anal. Chem. 2015, 87, 7250−7257